22

Demodulation Reference Signal Design and Channel Estimation for LTE-Advanced Uplink

Xiaolin Hou and Hidetoshi Kayama
DOCOMO Beijing Communications Laboratories Co., Ltd.
China

1. Introduction

The merits of 3GPP long term evolution (LTE), such as high spectral efficiency, very low latency, support of variable bandwidth, simple architecture, etc, make it the most competitive candidate for the next generation mobile communications standard. In the first release of LTE, only single transmit antenna is supported in the uplink due to its simplicity and acceptable performance. However, in order to keep its current leading position, LTE needs further evolvement (known as LTE-Advanced (LTE-A)) to provide better performance, including a higher uplink spectrum efficiency. Therefore, multiple transmit antennas must be supported in the LTE-A uplink and one important issue is the uplink demodulation reference signal (DMRS) design, which will influence uplink channel estimation accuracy and eventually determine uplink reliability and throughput.

In this study we first briefly review the current status of DMRS in LTE uplink and then different DMRS enhancement schemes are investigated for LTE-A uplink multiple-input multiple-output (MIMO) transmission. Also, two-dimensional channel estimation algorithms are provided to realize accurate uplink channel estimation. With computer simulations, the performances of several candidate LTE-A uplink DMRS design schemes are evaluated and compared. Finally some basic conclusions are provided together with the latest standardization progress.

2. DMRS in LTE uplink

LTE uplink is based on single-carrier frequency division multiple access (SC-FDMA) due to its low peak-to-average power ratio (PAPR). There are two types of reference signal in LTE uplink: DMRS used for data reception and sounding reference signal (SRS) used for scheduling and link adaptation. In this study we only focus on DMRS design and related channel estimation for the physical uplink shared channel (PUSCH).

Take frame structure type 1 for example, each LTE radio frame is 10ms long and consists of 20 slots of length 0.5ms. A subframe is defined as two consecutive slots. For the normal cyclic prefix (CP) case, each slot contains 7 symbols. The two-dimensional time-frequency resource can be partitioned as resource blocks (RBs) and each RB corresponds to one slot in the time domain and 180 kHz in the frequency domain. In LTE uplink, the DMRS for PUSCH in the frequency domain will be mapped to the same set of physical resource blocks (PRBs) used for the corresponding PUSCH transmission with the same length expressed by the number of

subcarriers, while in the time domain DMRS will occupy the $4th$ SC-FDMA symbol in each slot for the normal CP case, as shown in Fig. 1.

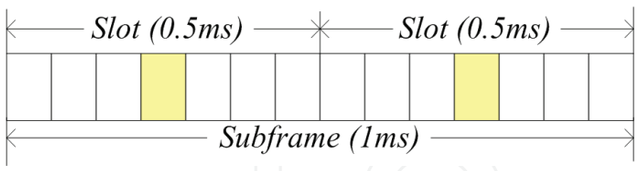

Fig. 1. DMRS in LTE uplink

In order to support a large number of user equipments (UEs) in multiple cells, a large number of different DMRS sequences are needed. A DMRS sequence $r_{u,v}^{(\alpha)}(n)$ is defined by a cyclic shift (CS) α of a base sequence $\bar{r}_{u,v}(n)$ according to

$$r_{u,v}^{(\alpha)}(n) = e^{j\alpha n} \cdot \bar{r}_{u,v}(n), 0 \leq n < M_{sc}^{RS} \tag{1}$$

where $M_{sc}^{RS} = mN_{sc}^{RB}$ is the length of DMRS sequence, m is the RB number and N_{sc}^{RB} is the subcarrier number within each RB. When the subcarrier bandwidth is set as 15kHz, each RB will contain 12 subcarriers, i.e., N_{sc}^{RB} = 12. Multiple DMRS sequences can be derived from a single base sequence through different values of α.

The definition of the base sequence depends on the sequence length. For $M_{sc}^{RS} \geq 3N_{sc}^{RB}$, the base sequence is defined as the cyclic extension of the Zadoff-Chu sequence (Chu, 1972)

$$\bar{r}_{u,v}(n) = x_q(n \bmod N_{ZC}^{RS}), 0 \leq n < M_{sc}^{RS} \tag{2}$$

$$x_q(m) = e^{-j\frac{\pi qm(m+1)}{N_{ZC}^{RS}}}, 0 \leq m < N_{ZC}^{RS} - 1 \tag{3}$$

where $x_q(m)$ is the q_{th} root Zadoff-Chu sequence and N_{ZC}^{RS} is the length of Zadoff-Chu sequence that is given by the largest prime number such that $N_{ZC}^{RS} < M_{sc}^{RS}$. For $M_{sc}^{RS} < 3N_{sc}^{RB}$, the base sequence is defined as the computer generated constant amplitude zero autocorrelation (CG-CAZAC) sequence

$$\bar{r}_{u,v}(n) = e^{j\varphi(n)\pi/4}, 0 \leq n < M_{sc}^{RS} \tag{4}$$

where the values of $\varphi(n)$ are given in (3GPP, TS 36.211).

Base sequences $\bar{r}_{u,v}(n)$ are divided into 30 groups with $u \in \{0, 1, ..., 29\}$. Each group contains one base sequence $(v = 0)$ with $1 \leq m \leq 5$ and two base sequences $(v = 0, 1)$ with $6 \leq m \leq N_{RB}^{max,UL}$, where $N_{RB}^{max,UL}$ is the maximum RB number in the uplink. In order to reduce inter-cell interference (ICI), neighboring cells should select DMRS sequences from different base sequence groups. Furthermore, there are 3 kinds of hopping defined for the DMRS in LTE uplink, i.e., group hopping, sequence hopping and CS hopping, where CS hopping should always be enabled in each slot.

The CS value α in a slot is given by $\alpha = 2\pi n_{cs}/12$ with

$$n_{cs} = (n_{DMRS}^{(1)} + n_{DMRS}^{(2)} + n_{PRS})/12 \tag{5}$$

where $n_{DMRS}^{(1)}$ is a broadcast value, $n_{DMRS}^{(2)}$ is included in the uplink scheduling assignment and n_{PRS} is given by a cell-specific pseudo-random sequence. Obviously, there are 12 usable CS values in total for DMRS in LTE uplink.

3. DMRS design and channel estimation for LTE-A uplink

3.1 DMRS enhancement

Current LTE uplink DMRS only considers UE with single transmit antenna. However, in order to boost the uplink spectrum efficiency, multiple transmit antennas must be supported in LTE-A uplink. Therefore, the uplink DMRS must be enhanced for MIMO transmission and each UE now may have multiple DMRS sequences, depending on its transmit antenna number (without precoding) or spatial layer number (with precoding).

There are several possible solutions, including CS extension, orthogonal cover code (OCC), interleaved frequency division multiplexing (IFDM) and their combinations. Considering the backwards compatibility with LTE and the low PAPR requirement for uplink transmission, IFDM should be excluded first. Then CS, OCC and their combinations are promising candidates for DMRS enhancement and will be discussed in more details in the following text.

3.1.1 Baseline: CS extension

Considering the backwards compatibility, it is agreed that cyclic shift separation is the baseline for the LTE-A uplink DMRS enhancement (3GPP, TR 36.814). Without loss of generality, uplink precoding is not considered in the following text, therefore, transmit antenna and spatial layer are equivalent and interchangeable. For single-user MIMO (SU-MIMO) transmission with $n_T \geq 2$ spatial layers, it is natural to assign multiple CS values to separate the multiple spatial layers. Then the questions remained to be answered are how to assign different CS values to different spatial layers and how to ensure the backwards compatibility to LTE.

If we assign multiple CS values with the following constraint

$$n_{cs,i} = (n_{cs,0} + \frac{C}{n_T} \cdot i) \bmod (C), i = 0, 1, ..., n_T - 1 \tag{6}$$

where $n_{cs,i}$ corresponds to the CS value of DMRS for the ith spatial layer and C is the constant value 12 for PUSCH. Then the CS value of DMRS for the first spatial layer $\alpha_0 = 2\pi n_{cs,0}/12$ is exactly the same as that for the single transmit antenna case in LTE. Therefore, all the original CS signaling and hopping designs for the single transmit antenna UE in LTE can be kept unchanged for the multiple transmit antennas UE in LTE-A, once the constraint in Eq. (6) is satisfied.

Because this DMRS design can be viewed as binding together the CS values of DMRS as well as the channel impulse response (CIR) positions of different spatial layers with the maximum distance constraint, as illustrated in Fig. 2 (Note that the relationship between α_i and α_0 will keep unchanged during CS hopping), we simply call it maximum distance binding (MDB).Its benefits include:

- First, the distance between CIRs of different spatial layers in the time domain can be always maximized, thus the interference between DMRS of different spatial layers can be minimized;
- Second, no additional signaling is required for CS notification and hopping when support uplink MIMO transmission, therefore, it is completely backwards compatible to LTE;
- Third, it can support time-domain inter-slot interpolation that is necessary for moderate to high mobility cases.

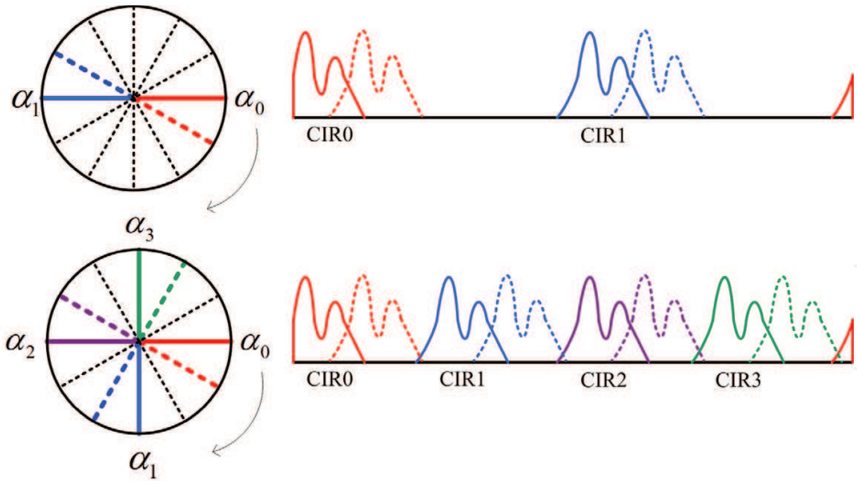

Fig. 2. CS extension with MDB

Actually, the same DMRS design principle can also be applied to the uplink multi-user MIMO (MU-MIMO) transmission with single transmit antenna UEs. Now it only requires some constraint in the uplink scheduling assignment for the CS values of multiple DMRS (because $n_{DMRS}^{(1)}$ and n_{PRS} are the same for all the UEs in the same cell, respectively) as follows

$$n_{DMRS,i}^{(2)} = (n_{DMRS,0}^{(2)} + \frac{C}{n_T} \cdot i) \bmod (C), i = 0, 1, ..., n_T - 1 \tag{7}$$

where $n_{DMRS,0}^{(2)}$ is the scheduled value for the first UE.
In order to support the above CS scheduling constraint for MU-MIMO transmission, we have two possible options:

- Option 1: No signaling modification
  Because the current LTE specification only supports 8 possible values for $n_{DMRS}^{(2)}$ (3GPP, TS 36.211), a limited number of combinations can be chosen in the uplink scheduling with the MDB constraint (7) satisfied. Therefore, for the 2-user case, $n_{DMRS,i}^{(2)} \in \{(0,6),(2,8),(3,9),(4,10)\}$; while for the 4-user case, $n_{DMRS,i}^{(2)} \in \{(0,3,6,9)\}$.
- Option 2: Slight signaling modification
  If the specific field in downlink control information (DCI) format 0 for the CS of DMRS can be increased from 3 bits to 4 bits, all the possible combinations in the CS scheduling for MU-MIMO transmission can be supported with the MDB constraint (7) satisfied.

3.1.2 Further enhancement: CS + OCC

For high-order SU-MIMO, MU-MIMO and coordinated multi-point (CoMP) reception that will be supported in the further evolvement of LTE, the number of superposed spatial layers will increase to four or even eight. In order to reduce the interference between multiple spatial layers, OCC, such as $[+1,+1]$ and $[+1,-1]$, can be further introduced across the two DMRS symbols within the same subframe.
For MU-MIMO and CoMP reception, CS + OCC can provide some special advantage compared to CS only scheme, such as capability to multiplex UEs with different transmit bandwidths and robustness to timing difference of multiple UEs. For SU-MIMO, CS + OCC

may also be attractive for high-order MIMO transmission and/or high-order modulation. The combination of CS and OCC could have two variations, i.e., CS + OCC with identical CS and CS + OCC with offset CS (TI, 2009), as illustrated in Fig. 3 (a) and Fig. 3 (b), respectively, taking four spatial layers for example.

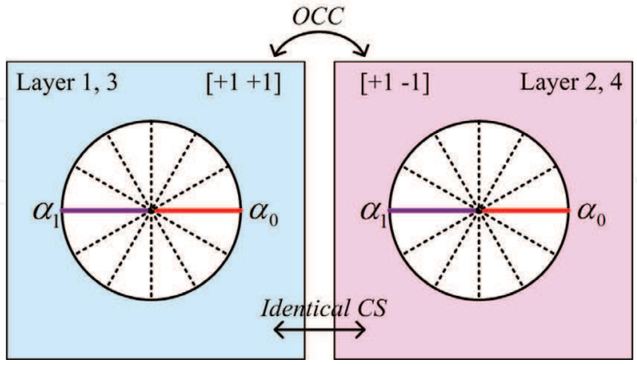

(a) CS + OCC

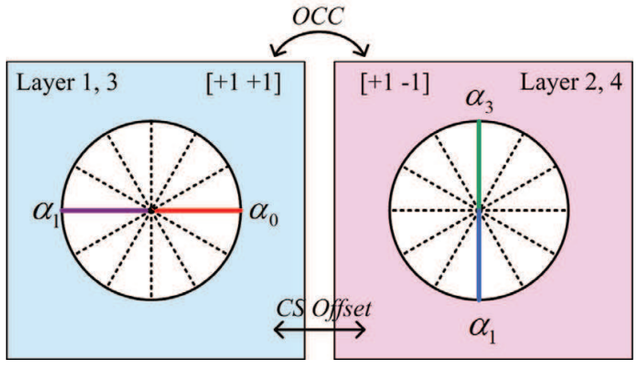

(b) CS + OCC (offset)

Fig. 3. Combination of CS and OCC

However, OCC will lose its effectiveness in some cases, such as when the mobility increases from low to moderate or PUSCH hopping happens within one subframe. In the aforementioned situations, CS + OCC with identical CS, abbr. as CS + OCC, cannot work at all; while CS + OCC with offset CS , abbr. as CS + OCC (offset), still can work, but in essence only CS takes effect now. Obviously, CS + OCC (offset) occupies twice CS resources compared to CS + OCC. Meanwhile, to introduce OCC into LTE-A uplink DMRS design, some additional control signaling may be needed. Otherwise, the linkage between OCC and CS must be defined to avoid increasing control signaling, i.e., the notification of OCC could be realized in an explicit way.

3.2 Two-dimensional channel estimation

In order to obtain the time-frequency two-dimensional channel state information (CSI) in the SC-FDMA uplink, two-dimensional channel estimation is needed for each subframe. Without loss of generality, assume that the inter-symbol interference (ISI) and the inter-carrier interference (ICI) are small and neglectable. Therefore, for PDSCH and corresponding DMRS

within one subframe, the received signal at the k-th subcarrier in the l-th SC-FDMA symbol can be written as

$$Y(k,l) = H(k,l) \cdot X(k,l) + N(k,l), k_0 \leq k < k_0 + 12 \cdot N_{RB}^{UL} - 1, 0 \leq l < 14 \tag{8}$$

where $X(k,l)$, $H(k,l)$ and $N(k,l)$ denote the transmitted signal, the channel frequency response (CFR) and the additive white Gaussian noise (AWGN) with zero mean and variance σ^2 for the k-th subcarrier in the l-th SC-FDMA symbol, respectively. k_0 is the frequency starting position of PUSCH and N_{RB}^{UL} is the uplink RB number for PUSCH. For the multipath wireless channel within one SC-FDMA symbol, the CFR can be related to the CIR as

$$H(k,l) = \sum_{g=0}^{G-1} h(g,l) \cdot e^{-j2\pi kg/K} \tag{9}$$

where $h(g,l)$ is the g-th multipath component and G is the sample number corresponding to the maximum multipath delay.

The first step of two-dimensional channel estimation is to obtain the initial estimated superposed channels within the two DMRS symbols, i.e., $\hat{H}(k,3)$ and $\hat{H}(k,10)$, as follows

$$\hat{H}(k,l) = Y(k,l) \cdot conj(r_{u,v}^{(\alpha_0)}(k)), l = 3, 10 \tag{10}$$

where $conj(\cdot)$ represents the complex conjugate and without loss of generality, PUSCH and DMRS hopping are not considered.

To facilitate the following description, define the final estimated channel as $\tilde{H}(k,l)$. Then the target of two-dimensional channel estimation is to derive each data symbol's $\tilde{H}(k,l)$ from $\hat{H}(k,3)$ and $\hat{H}(k,10)$. Taking the implementation complexity into account, two concatenated one-dimensional channel estimation, i.e., frequency-dimensional channel estimation and time-dimensional channel estimation, will be considered in this study.

3.2.1 Frequency-dimensional channel estimation

For frequency-dimensional channel estimation, discrete-time Fourier transform (DFT) based channel estimation (Edfors et al., 2000) could be utilized. However, because the RB allocation to a given UE is generally only a small portion of the overall uplink bandwidth, the CIR energy leakage will be observed in practice, as shown in Fig. 4, where the first and the second rows are for two-antenna and four-antenna cases, while the left and the right columns are for RB# = 1 and RB# = 10 cases, respectively. It's obvious that the smaller the RB number, the more severe the CIR energy leakage. This phenomenon will make the CIRs from different transmit antennas superposed together and difficult to be separated with each other, especially when the transmit antenna number becomes larger. Furthermore, the frequency domain Gibbs phenomenon (Oppenheim et al., 1999) will appear at the edges of assigned consecutive RBs for a given UE due to the signal discontinuities. Therefore, the estimation accuracy of traditional DFT-based channel estimation will deteriorate significantly in practice.

In order to mitigate the aforementioned problems, an improved DFT-based channel estimation was proposed for LTE(-A) uplink (Hou et al., 2009), which is illustrated in Fig. 5 for each receive antenna of eNB. After serial-to-parallel (S/P) conversion and K-point fast Fourier transform (FFT), the received signal is transformed into the frequency domain. Because each UE (except for UEs in the same MU-MIMO transmission) occupies different RBs in the uplink, we can first separate different UEs by way of frequency division multiplexing (FDM). Then taking channel estimation for UE1 for example, multiply the separated received DMRS by

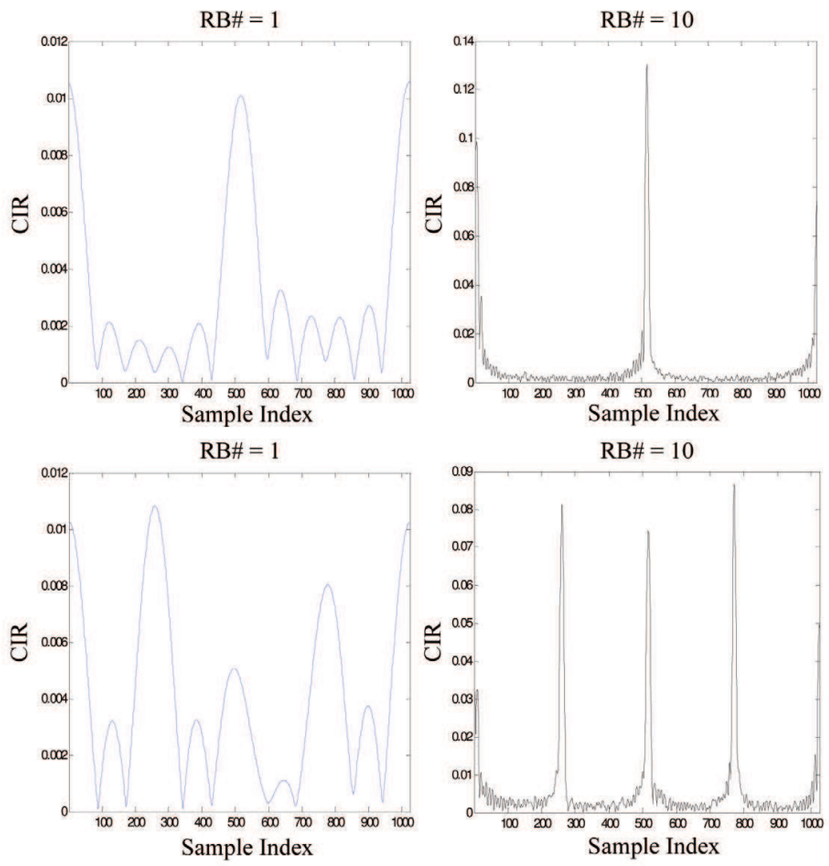

Fig. 4. CIR energy leakage

the complex conjugate of the DMRS sequence assigned for the 1st spatial layer and perform K-point inverse FFT (IFFT) to get the superposed CIRs in the time domain, i.e.,

$$\hat{h}(g,l) = ifft(\hat{H}(k,l)), 0 \leq k < K, l = 3, 10 \tag{11}$$

After the operation of dynamic CIR reservation (DCIR^2), we can seperate the CIRs for different spatial layers by way of different CS values. As for the operation of DCIR^2, the dynamically reserved CIR for each spatial layer consists of 2 parts with respect to the timing positions, i.e., $(\frac{C}{n_T} \cdot i) \cdot K, i = 0, 1, ..., n_T - 1$:

- Right part
  There are $\lambda \cdot CP$ samples preserved with the following right boundary

$$(\frac{C}{n_T} \cdot i) \cdot K + \lambda \cdot CP - 1, i = 0, 1, ..., n_T - 1 \tag{12}$$

  where CP is the cyclic prefix length of the SC-FDMA symbol and λ is an adjustable parameter ($0 \leq \lambda < 1$) that can be optimized in practical implementations.

- Left part
  There are $\mu \cdot \Delta$ samples preserved with the following left boundary

$$[(\frac{C}{n_T}\cdot i)\cdot K-\mu\cdot\Delta+K]\mathrm{mod}(K), i=0,1,...,n_T-1 \tag{13}$$

where Δ is the main lobe width of CIR energy leakage ($\Delta=\frac{K}{12\cdot RB\#}$) and μ is an adjustable parameter ($0\leq\mu<\frac{K/n_T-CP}{\Delta}$) that can be optimized in practical implementations. In order to simply the adjustment, we can define $\tilde{\Delta}=\frac{K}{12}$ and $\tilde{\mu}=\frac{\mu}{RB\#}$, therefore, $\tilde{\Delta}$ becomes a constant and only $\tilde{\mu}$ should be adjusted.

The proper choices of λ and $\tilde{\mu}$ are mainly determined by the noise level, the multipath delay profile and the assigned RB number for a given UE. And afer DCIR[2], we can obtain the CIR for the i-th spatial layer as $\tilde{h}_i(g,l)$.
Finally, the frequency-dimensional channel estimation result of DMRS symbols for the i-th spatial layer can be achieved by K-point FFT and provided to the following time-dimentional channel estimation block.

$$\tilde{H}_i(k,l)=ifft(\tilde{h}_i(g,l)), 0\leq g<K, l=3,10 \tag{14}$$

Another point should be emphasized is the operation of frequency domain windowing/dewindowing . Due to the frequency domain Gibbs phenomenon caused by the discontinuities at the edges of assigned consecutive RBs for a given UE, the overall channel estimation accuracy will be degraded, especially at the edges of assigned consecutive RBs. Therefore, some frequency domain window, such as Hanning window, Hamming window, Blackman window, etc. (Oppenheim et al., 1999), can be further added (see the dashed-line blocks in Fig. 5) to improve the channel estimation accuracy with some additional complexity. For example, Blackman window will be adopted in our following computer simulations.

$$w(n)=0.42-0.5cos(2\pi n/M)+0.08cos(4\pi n/M) \tag{15}$$

where M is the window length and $0\leq n\leq M$. In order not to eliminate the useful signals within the assigned RBs, the window length should be larger than the assigned bandwidth ($12\cdot RB\#$) for the corresponding UE.
Note that the improved DFT-based channel estimation can be applied to not only LTE-A MIMO uplink, but also LTE single-input single-output (SISO) or single-input multiple-output (SIMO) uplink.

3.2.2 Time-dimensional channel estimation

After frequency-dimensional channel estimation, we only obtain channel estimation results for two DMRS symbols within each subframe. In order to further acquire channel estimation result for each data symbol, time-dimensional channel estimation is needed, i.e., inter-slot interpolation via two DMRS symbols within each subframe. Two practical schemes are time-dimensional linear interpolation (TD-LI) and time-dimensional average or despreading (TD-Average/Despreading), i.e.,

$$\tilde{H}(k,l)=c_l\cdot\tilde{H}(k,3)+(1-c_l)\cdot\tilde{H}(k,10), 0\leq l<14 \tag{16}$$

$$\begin{aligned} c_l&=(10-l)/7 \quad , \quad TD-LI \\ c_l&=1/2 \quad , \quad TD-Average \end{aligned} \tag{17}$$

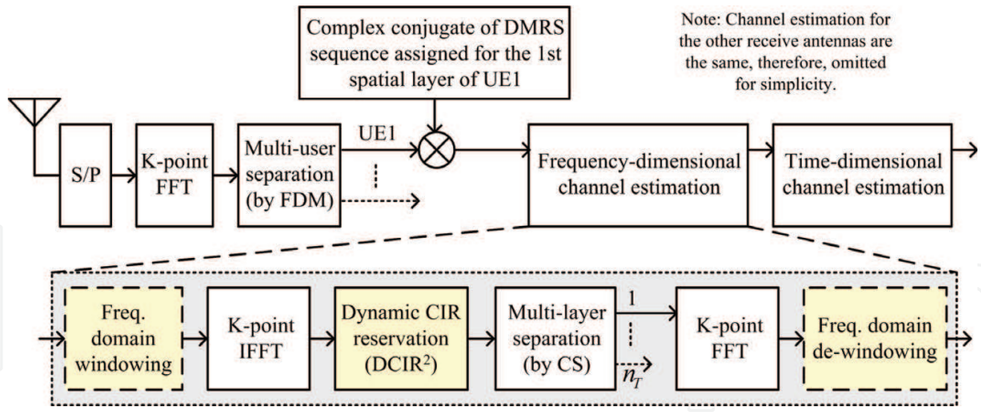

Fig. 5. The improved DFT-based channel estimation

It should be noted that for the case of CS + OCC with identical CS, TD-Despreading must be carried out before frequency-dimensional channel estimation.

4. Performance evaluation

Computer simulation results, including both block error rate (BLER) and throughput performances, will be provided in this section to compare different DMRS design schemes, i.e., CS only, CS + OCC and CS + OCC (offset).

The simulation parameters are listed in Table 1. Notice that the FFT size is larger than the usable subcarrier number because of the existence of guard band. There are totally 50 RBs in the uplink and we consider two RB# allocation cases with RB# $= 4, 10$, respectively. Furthermore, 2 typical MIMO configurations, i.e., 2×2 and 4×4, are both simulated. The MIMO transmission scheme is spatial multiplexing without precoding and the MIMO detection scheme is minimum mean square error (MMSE) detection. Without loss of generality, synchronization error and PUSCH hopping are not considered. For the improved DFT-based frequency-dimensional channel estimation, we simply chose $\lambda = 0.5$ and $\tilde{\mu} = 0.2$ and the frequency domain window length is set to be $M = 1.1 \cdot RB\# \cdot 12$. The channel model is selected as typical urban (TU) with mobility of 3km/h or 30km/h.

First, BLER performances of different DMRS design schemes will be compared. The same frequency-dimensional channel estimation is utilized for different DMRS design schemes and time-dimensional channel estimation could be different, i.e., CS + OCC can only use TD-Despreading, while CS only and CS + OCC (offset) can use TD-LI or TD-Average/Despreading. Furthermore, the curve with perfect CSI is also provided in each figure for comparison. The BLER performances are evaluated with two representative configurations, i.e., 10RB with 16QAM and 4RB with 64QAM (the coding rate is 1/2), for 2×2 and 4×4 MIMO, respectively.

When the mobile speed is as low as 3km/h, Fig. 6 shows that for the 2×2 MIMO case different DMRS design schemes have almost the same BLER performance. The only difference comes from time-directional channel estimation, i.e., TD-Average/Despreading can achieve slightly better performance than TD-LI due to the noise averaging effect in low mobility cases. And from Fig. 7, it can be observed that for the 4×4 MIMO case the introduction of OCC is helpful to improve the BLER performance in low mobility cases, especially when the RB number is small and/or the modulation order is high.

Parameters	Values
Carrier frequency	2GHz
Bandwidth	10MHz
FFT size	1024
Usable subcarrier #	600
Cyclic prefix	72
Assigned RB #	4, 10
MIMO configuration (Spatial multiplexing)	2×2 4×4
MIMO detection	MMSE
Modulation	QPSK,16QAM,64QAM
Channel coding	Turbo (Coding rate 1/2, 2/3, 3/4)
Synchronization	Perfect
PUSCH hopping	Disabled
DMRS design	CS Only CS + OCC CS + OCC (offset)
Frequency-dimensional channel estimation	Improved DFT-based
Time-dimensional channel estimation	TD-LI TD-Average/TD-Despreading
Channel model	Typical Urban (TU)
Mobile speed	3km/h, 30km/h

Table 1. Simulation parameters

However, if the mobile speed increases from low to moderate, i.e., from 3km/h to 30km/h, the aforementioned conclusion has to be revised. As shown in Fig. 8, now CS only with TD-LI can achieve the best performance and OCC will lose its effectiveness. The reason behind is that when the mobile speed is as high as 30km/h, the wireless channels between two consecutive slots are relatively fast time-varying, which makes TD-Average/Despreading cannot work well. On the other hand, TD-LI can still track the time-varying channel effectively. Therefore, from the mobility point of view, OCC has its apparent limitation, i.e., OCC will mainly work in the low mobility cases. However, considering the major application scenario of MIMO is the low mobility environment, OCC is still attractive for DMRS enhancement. And in the following simulations only 3km/h is considered.

In order to provide a more comprehensive comparison between different DMRS design schemes, the throughput performances with different modulation level and coding rate are provided in Fig. 9 and Fig. 10 for 2×2 and 4×4 MIMO, respectively. Three different modulation schemes (QPSK, 16QAM, 64QAM) and three different coding rates (1/2, 2/3, 3/4) are simulated, so in total there are nine combinations of modulation and coding. Considering the mobile speed is low, TD-Average/Despreading will be adopted instead of TD-LI. Also under this situation, because CS + OCC and CS + OCC (Offset) have neglectable performance difference, only CS + OCC is simulated, together with CS only and perfect CSI. Therefore, in each figure there are 27 curves, shown by different line styles and markers. For each DMRS design scheme, only the envelop of nine curves (each with one specific combination of modulation and coding) is highlighted to show the highest achievable throughput, which

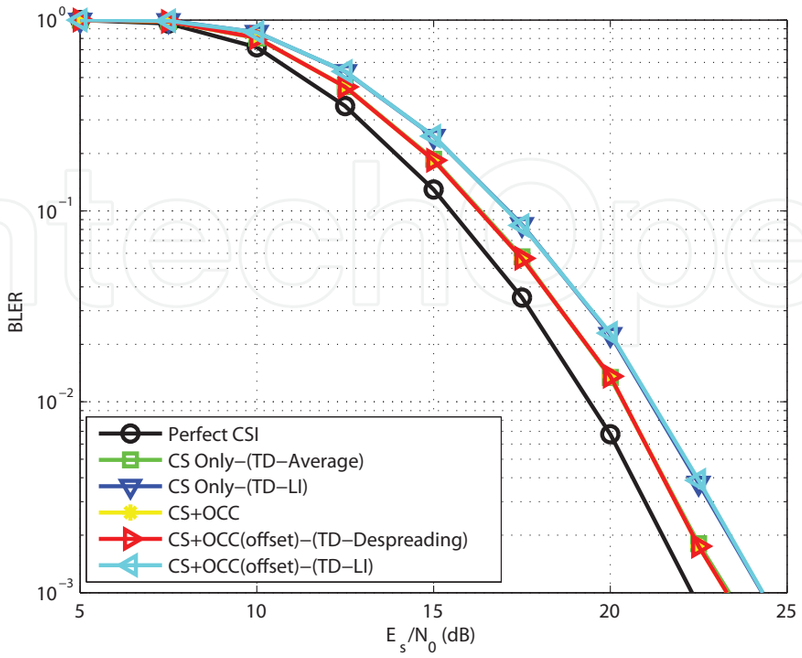

(a) 10RB, 16QAM

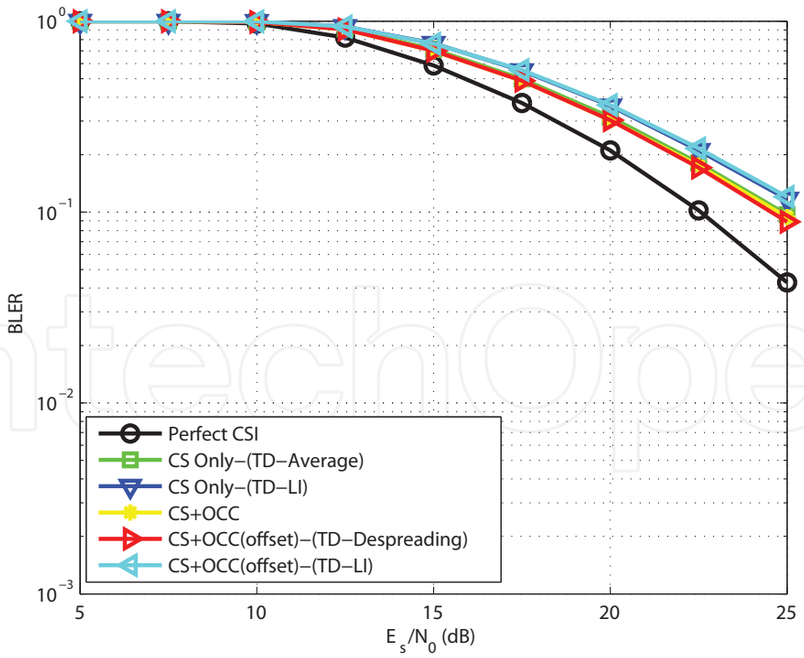

(b) 4RB, 64QAM

Fig. 6. BLER performance (2×2 MIMO, TU, 3km/h)

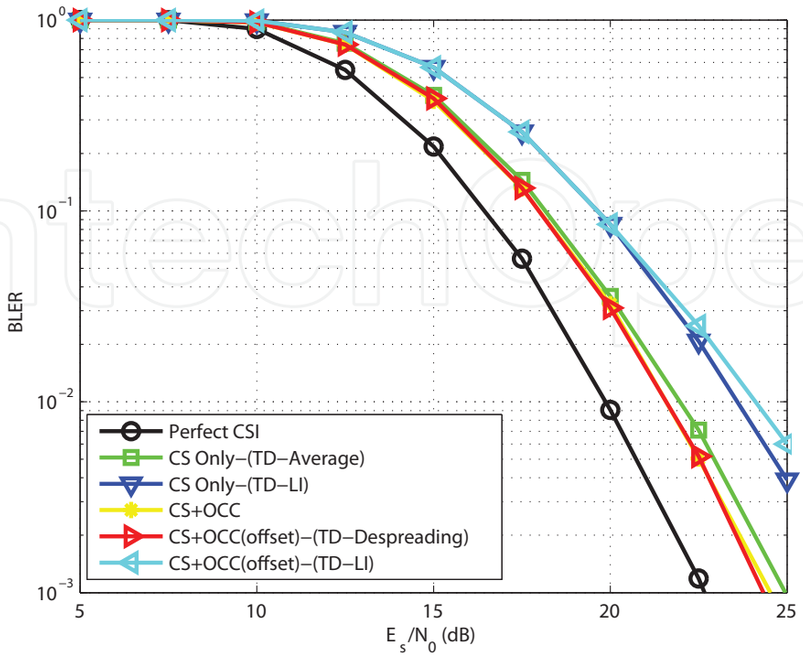

(a) 10RB, 16QAM

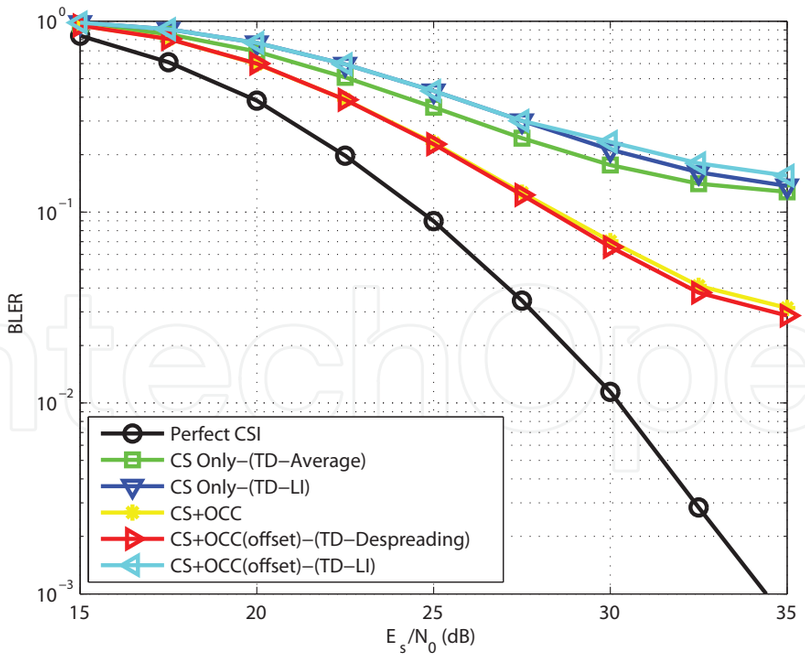

(b) 4RB, 64QAM

Fig. 7. BLER performance (4×4 MIMO, TU, 3km/h)

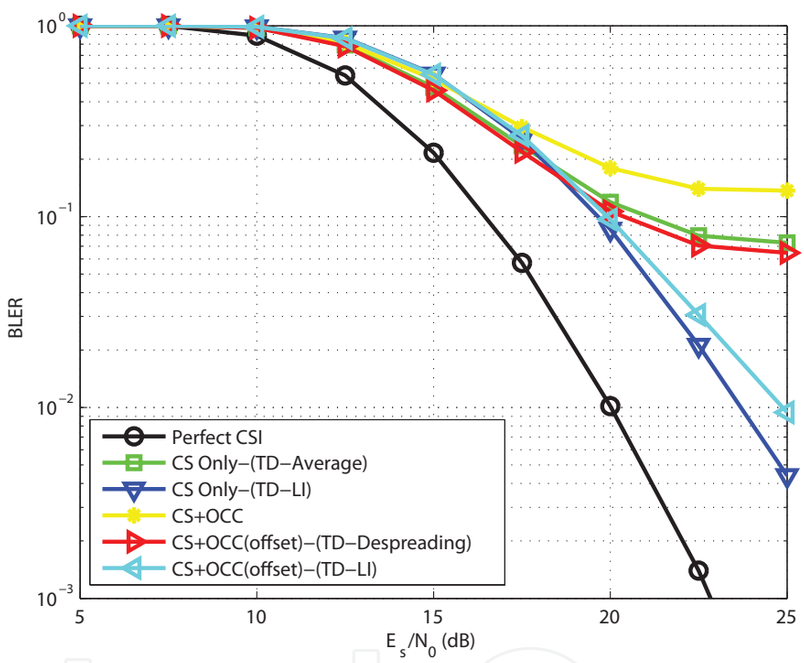

Fig. 8. BLER performance (4×4 MIMO, 10RB, 16QAM, TU, 30km/h)

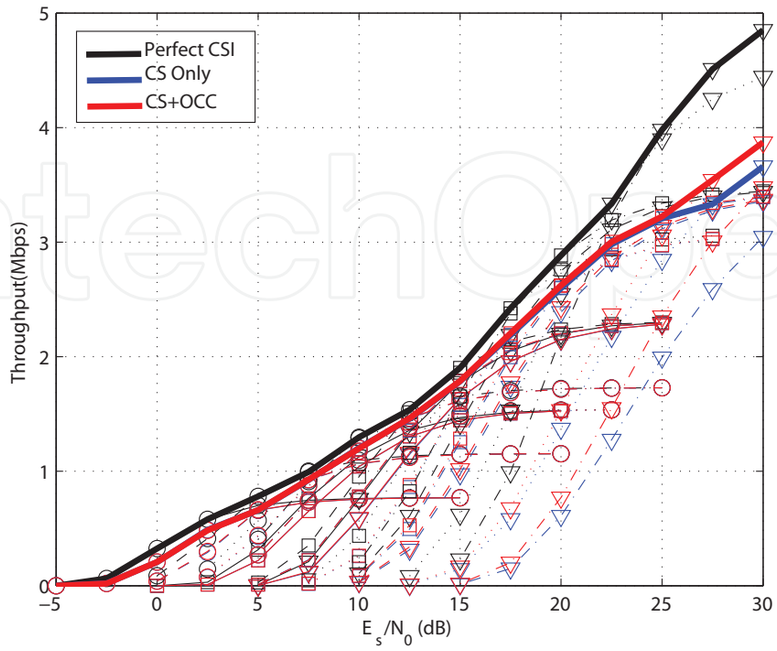

(a) 4RB

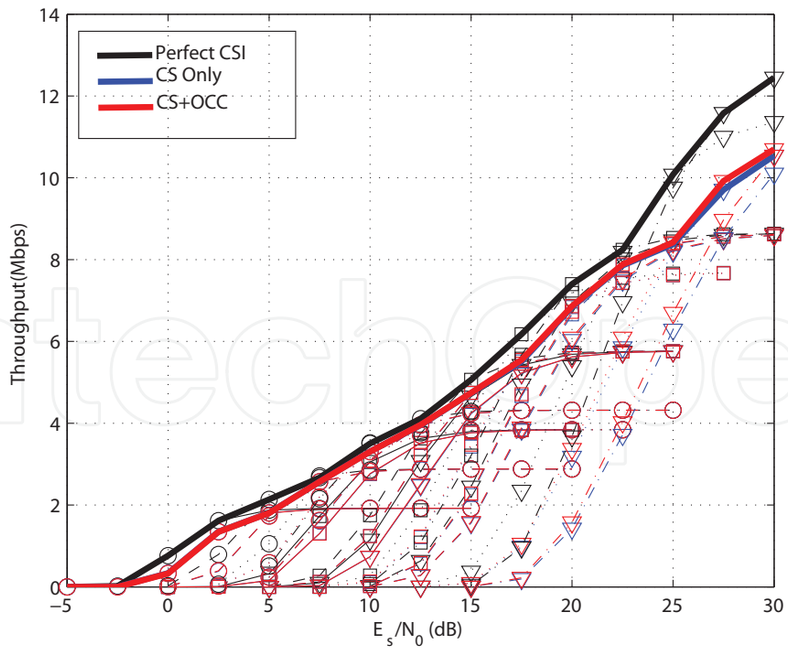

(b) 10RB

Fig. 9. Throughput performance (2×2 MIMO, TU, 3km/h)

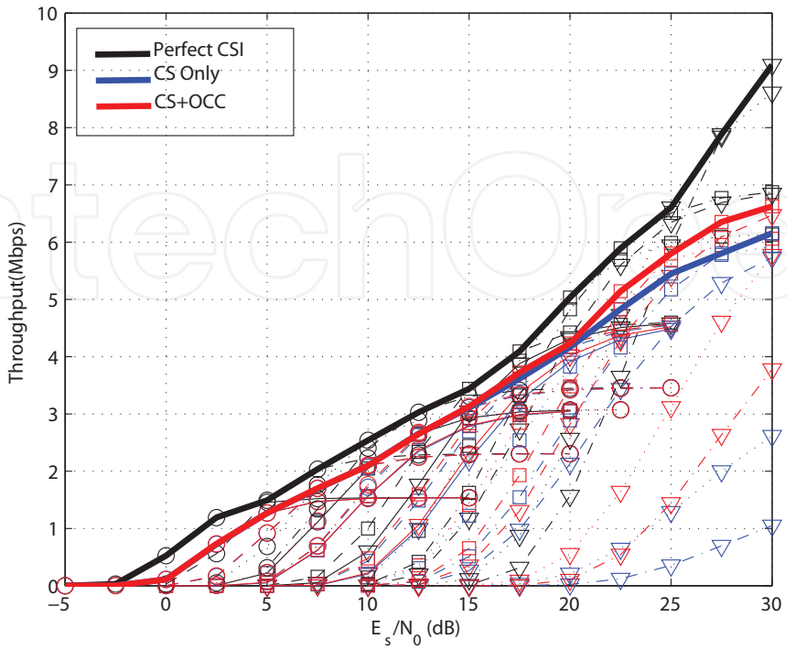

(a) 4RB

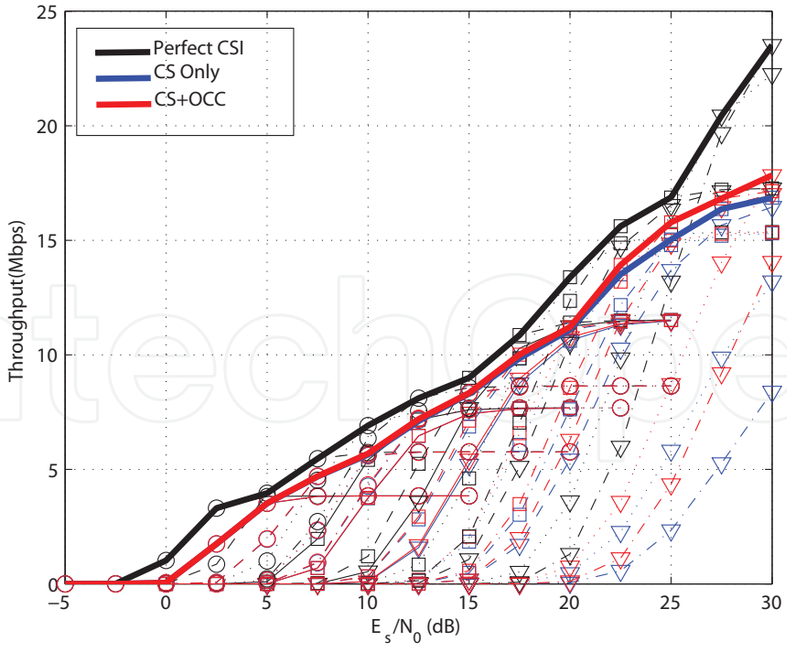

(b) 10RB

Fig. 10. Throughput performance (4×4 MIMO, TU, 3km/h)

could be viewed as the throughput performance with the ideal adaptive modulation and coding. From Fig. 9 and Fig. 10, we can observe that the introduction of OCC can improve throughput to some extent when some of the following situations are satisfied, i.e., the antenna number is large, the RB number is small, and the sigal-to-noise ratio is high.

5. Some basic conclusions and standardization progress

DMRS enhancement is a key step to support MIMO transmission, including SU-MIMO, MU-MIMO and CoMP, for LTE-A uplink. In this study different DMRS design schemes as well as channel estimation are investigated. In addition to the baseline of CS extension, the further combination of CS with OCC is also discussed. In addition to the special advantage for MU-MIMO and CoMP, CS + OCC is also attractive for high-order SU-MIMO to further suppress the interferences among the increasing multiple spatial layers. With the enhanced DMRS design and improved channel estimation, a higher spectrum efficiency can be realized in LTE-A uplink. Meanwhile, considering the backwards compatibility, as less as possible modification to the current LTE specification is preferred.
In the recent 3GPP RAN1 meetings, it was agreed that (3GPP, R1-102601)

- Introduce the OCC in Rel-10 without increasing uplink grant signaling overhead
- OCC can be used for both SU-MIMO and MU-MIMO

More design details about DMRS enhancement, such as CS and OCC linkage, DMRS hopping, etc., are still under discussions and hopefully the uplink DMRS enhancement for LTE-A will be finalized by the end of 2010.

6. References

3GPP. R1-102601: Final report of 3GPP TSG RAN WG1 #60bis, *3GPP TSG RAN WG1 Meeting #61*, Montreal, Canada, May 10-14, 2010.

3GPP TR 36.814 *http://www.3gpp.org/ftp/specs/html-info/36814.htm*

3GPP TS 36.211 *http://www.3gpp.org/ftp/specs/html-info/36211.htm*

Chu, D. C. (1972). Polyphase codes with good periodic correlation properties. *IEEE Trans. Info. Theory*, Vol. 18, No. 4, July 1972, pp. 531-532, ISSN 0018-9448

Edfors, O.; Sandell, M.; van de Beek, J. J.; Wilson, S. K. & Borjesson, P. O. (2000). Analysis of DFT-based channel estimators for OFDM. *Wireless Pers. Commun.*, Vol. 12, No. 1, Jan. 2000, pp. 55-70, ISSN 0929-6212

Hou, X.; Zhang, Z. & Kayama, H. (2009). DMRS design and channel estimation for LTE-Advanced MIMO uplink, *Proc. IEEE VTC09-Fall*, Alaska, USA, Sept. 20-23, 2009.

Oppenheim, A. V.; Schafer, R. W. & Buck, J. R. (1999). *Discrete-Time Signal Processing, 2nd ed.*, Prentice Hall, ISBN 013216292X, New Jersey

Texas Instruments. R1-091843: Discussion on UL DM RS for SU-MIMO, *3GPP TSG RAN WG1 Meeting #57*, San Francisco, USA, May 4-8, 2009.

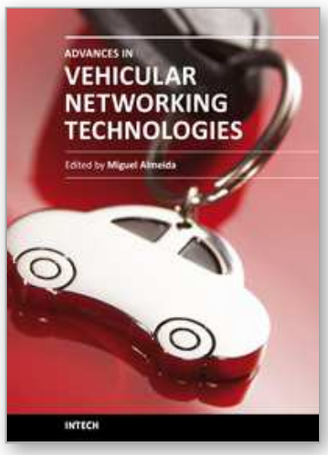

Advances in Vehicular Networking Technologies

Edited by Dr Miguel Almeida

ISBN 978-953-307-241-8
Hard cover, 432 pages
Publisher InTech
Published online 11, April, 2011
Published in print edition April, 2011

This book provides an insight on both the challenges and the technological solutions of several approaches, which allow connecting vehicles between each other and with the network. It underlines the trends on networking capabilities and their issues, further focusing on the MAC and Physical layer challenges. Ranging from the advances on radio access technologies to intelligent mechanisms deployed to enhance cooperative communications, cognitive radio and multiple antenna systems have been given particular highlight.

How to reference

In order to correctly reference this scholarly work, feel free to copy and paste the following:

Xiaolin Hou and Hidetoshi Kayama (2011). Demodulation Reference Signal Design and Channel Estimation for LTE-Advanced Uplink, Advances in Vehicular Networking Technologies, Dr Miguel Almeida (Ed.), ISBN: 978-953-307-241-8, InTech, Available from: http://www.intechopen.com/books/advances-in-vehicular-networking-technologies/demodulation-reference-signal-design-and-channel-estimation-for-lte-advanced-uplink

INTECH
open science | open minds

InTech Europe
University Campus STeP Ri
Slavka Krautzeka 83/A
51000 Rijeka, Croatia
Phone: +385 (51) 770 447
Fax: +385 (51) 686 166
www.intechopen.com

InTech China
Unit 405, Office Block, Hotel Equatorial Shanghai
No.65, Yan An Road (West), Shanghai, 200040, China
中国上海市延安西路65号上海国际贵都大饭店办公楼405单元
Phone: +86-21-62489820
Fax: +86-21-62489821

IntechOpen